Chinese Journal of Chemical Engineering 55 (2023) 1–12

Contents lists available at ScienceDirect

Chinese Journal of Chemical Engineering

journal homepage: www.elsevier.com/locate/CJChE

Full Length Article

Impacts of solid physical properties on the performances of a slurry external airlift loop reactor integrating mixing and separation

Tian Zhang [1,2], Qingshan Huang [2,3,4,5,6], Shujun Geng [2,3,4,5,6], Aqiang Chen [2,3,4,5,6], Yan Liu [1,*], Haidong Zhang [2,3,4,5,6,*]

[1] *School of Chemical Engineering, Hebei University of Technology, Tianjin 300130, China*
[2] *Key Laboratory of Biofuels, Qingdao Institute of Bioenergy and Bioprocess Technology (QIBEBT), Chinese Academy of Sciences (CAS), Qingdao 266101, China*
[3] *Dalian National Laboratory for Clean Energy (DNL), Dalian 116023, China*
[4] *Innovation Academy for Green Manufacture, Institute of Process Engineering, CAS, Beijing 100190, China*
[5] *Synthetic Biology Technology Innovation Center of Shandong Province, Qingdao 266101, China*
[6] *Shandong Energy Institute, Qingdao 266101, China*

A R T I C L E I N F O

Article history:
Received 14 December 2021
Received in revised form 30 April 2022
Accepted 8 May 2022
Available online 16 May 2022

Keywords:
Slurry reactor
Hydrodynamics
Particle
Mixing
Solid physical property

A B S T R A C T

Solid physical properties are vital for the design, optimization, and scale-up of gas–liquid–solid multiphase reactors. The complex and interactional effects of the solid physical properties, including particle diameter, density, wettability, and sphericity, on the hydrodynamic behaviors in a new external airlift loop reactor (EALR) integrating mixing and separation are decoupled in this work. Two semi-empirical equations are proposed and validated to predict the overall gas holdup and liquid circulating velocity satisfactorily, and then the individual influence of such solid physical properties is further investigated. The results demonstrate that both the overall gas holdup in the riser and the liquid circulating velocity in the downcomer increase with the contact angle, but decrease with particle size, density, and sphericity. Additionally, the impact of the particle size on the liquid circulating velocity is also profoundly revealed on a micro-level considering the particle size distribution. Moreover, the axial solid concentration distribution is discussed, and the uniformity of the slurry is described by the mixing index of the solid particles. The results show that a more homogeneous mixture can be achieved by adding finer particles other than attaining violent turbulence. Therefore, this work lays a foundation for the design, scale-up, and industrialization of the EALRs.

1. Introduction

Airlift loop reactor (ALR) is an efficient gas–liquid or gas–liquid–solid multiphase reactor developed from bubble column [1,2]. Compared to the traditional bubble columns, the ALRs have many advantages, such as unique directional flow, faster flow rate, and more uniform temperature distribution [3–5]. Moreover, ALRs have the superiorities of simple structure (no mechanical structure), low energy consumption (no additional energy input), outstanding mixing, excellent mass transfer efficiency (excellent interphase contact), and so on [6–8]. To date, the ALRs have been widely applied in many fields, such as the Fischer–Tropsch synthesis [9–11], wastewater treatment [12–14], diesel hydrodesulfurization [15], biological fermentation [7,16–19], direct coal liquefaction [5], cell culture [7,19,20], fine chemical industry [21–23], and so forth.

The hydrodynamic performance and mixing ability will be significantly influenced when solid particles are added to the gas–liquid systems. Many researchers [24–29] found that the transition of flow patterns, gas volume fraction, liquid circulation velocity, mass/heat transfer performance, bubble size and distribution, bubble rising velocity, and liquid viscosity in the gas–liquid system would change dramatically when the solid particles were added. This is crucial to the scale-up and industrialization of the ALRs since most of the application cases contain solid phases. Therefore, a deep understanding of solid particles' impacts is highly desired because of the multiple-property nature, and more and more attention has been attracted to study the effect of solid properties on the performances of ALRs in recent decades.

* Corresponding authors.
E-mail addresses: 1998033@hebut.edu.cn (Y. Liu), zhanghaidong@qibebt.ac.cn (H. Zhang).

https://doi.org/10.1016/j.cjche.2022.05.001

The mean diameter of the particles used in most slurry reactors usually ranges from 20 to 300 μm, and the size distribution always varies significantly, resulting in substantial differences in the hydrodynamics. Lakhdissi *et al.* [30,31] claimed that a bigger mean diameter of particles would reduce the overall gas holdup. They also found that the effect of the mean diameter of solid particles at the micron level on volumetric mass transfer coefficient (k_La) can be neglected under a relatively low solid volume concentration (1%–5%), and larger solid particles would lead to a more significant reduction in the overall gas holdup. Similar conclusions were also obtained by some other scholars [26,32–35], who also found a negative impact on the gas holdup with increasing particle diameter. However, some works showed a negligible influence of particle size on gas holdup in a relatively wide range of size distributions, *i.e.*, from 44 to 254 μm [36,37]. Li *et al.* [38] also stated that the particle size had little effect on flow regime transition with solid particle size ranging from 48 to 150 μm, while the flow could be promoted to a heterogeneous regime when the particle size was approaching 270 μm. Additionally, Sarhan *et al.* [39] even observed that the bubble coalescence was restrained by increasing particle size from 60 to 150 μm, leading to a higher gas holdup. It is seen that adequate studies on the influence of particle size on flow hydrodynamics are still lacking due to controversial conclusions.

Particle density usually plays a significant role in deciding the reactor type and operating conditions. Though it is verified that the particle density exerts remarkable influence on the gas holdup, the degree of coalescence, and the fluidization regime transition [38,40], some distinct conclusions also need to be concerned about. For example, Freitas *et al.* [41] investigated the influence of solid density on the gas holdup, circulation time, and liquid velocity in a three-phase external airlift loop reactor (EALR) and found that it had little influence on riser gas holdup and liquid velocity but a negative effect on circulation time. While Guo *et al.* [42] argued that after adding some solid particles into the gas–liquid two-phase system, the gas holdup would increase with increasing the concentration and density of solid particles, though the liquid circulating velocity behaved oppositely. Some opposite phenomena were also depicted by Jamialahmadi and Müller-Steinhagen [43], who believed that low-density particles would lead to a higher gas holdup. It seems that the particle density has a distinct influence on the flow hydrodynamics, and it would interact with operating parameters such as superficial gas velocity, temperature, *etc.* [38,40].

Besides, the influence of other particle properties on flow characteristics has been investigated, while different conclusions are drawn. Some researchers [43–46] studied the effect of wettability on gas holdup, stating that the non-wettable particles would decrease the gas holdup, while the wettable particles would increase it. However, some other people [36,47,48] came up with the opposite conclusion, and they concluded that the addition of wettable particles would reduce the gas holdup due to the strengthening bubble coalescence in the gas–liquid–solid systems.

Additionally, the influence of particle shape on the performances of such slurry systems should also be a concern due to the rich and complex variations of particle morphology. Sastaravet *et al.* [49] found that the k_La in bubble column reactors and airlift loop reactors with solid particles of different shapes (ring, sphere, cylinder, and cube) varied differently. Mena *et al.* [50] put forward that when adding solid particles with different surface properties into the bubble column, solid concentration behaved differently on k_La. The particle concentration also plays an essential role in the hydrodynamics of such multiphase reactors and has been studied extensively [51–54], while investigation concentrating on the particle physical properties is still lacking. What's more, the particle properties aforementioned may have no clear trend on the hydrodynamics, so it is fundamental to clarify the performances of such gas–liquid–solid three-phase reactors concerning the specific operating conditions.

In a word, a deep understanding of the influence of particle properties needs further verification from comprehensive studies to design optimum reactors and select optimal operating conditions for the slurry reactors. However, it is still difficult to investigate the individual effects of particle size, density, wettability, and sphericity on the hydrodynamic characteristics in such gas–liquid–solid systems due to their mutual dependence. To the best of our knowledge, there are no publications individually dealing with all the properties comprehensively and theoretically. Hence, the individual influence of the solid physical properties (*i.e.*, particle size, density, wettability, and sphericity) on the hydrodynamic performances in an EALR with broad application prospects [53] was revealed here for the first time by the unique combination of the experimental data and theoretical analysis. Three kinds of solid particles with different densities, mean diameters, contact angles, and sphericities were elaborately chosen, and their relative effects on overall gas holdup, liquid circulating velocity were explored. Moreover, the axial solid concentration distribution and the mixing characteristics were also analyzed to obtain a deep understanding of such slurry reactors and improve their performances for industrial production in the future.

2. Materials and Methods

2.1. Experimental setup and materials

The equipment taken in this experiment is a pilot new EALR, the schematic of which is shown as Fig. 1, and the structure details can be found in our previous work [53,55].

During the experiment, the gas enters the riser after being distributed by a sparger. The solid catalyst is automatically recycled into the riser from the downcomer *via* the hydrocyclone's underflow, and the clarified liquid products are discharged from the

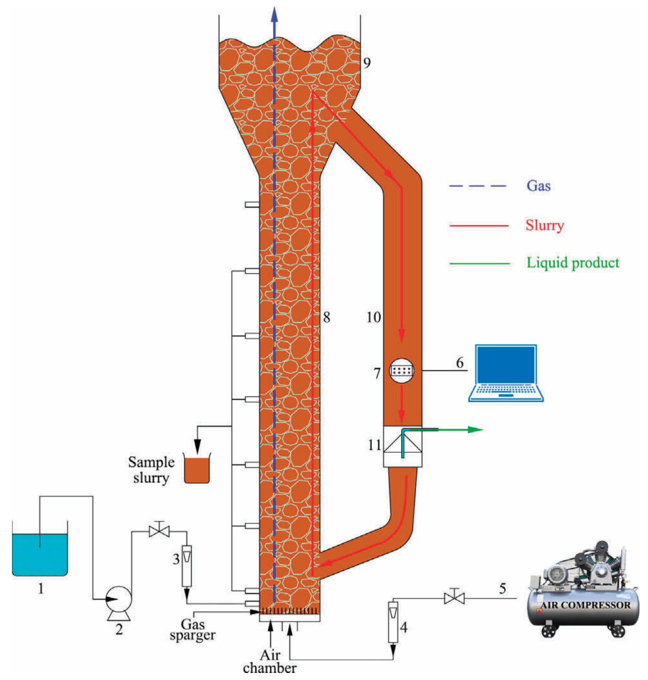

Fig. 1. The schematic of the experimental setup (1—liquid tank; 2—water pump; 3—liquid flow meter; 4—gas flow meter; 5—air compressor; 6—computer; 7—electromagnetic flow meter; 8—riser; 9—separator; 10—downcomer; 11—hydrocyclone).

overflow without any external force. The principle and advantages of the elaborately designed hydrocyclones are also comprehensively explained by Geng *et al.* [53]. In this work, the wall effects on the gas holdup can be ignored since the column diameter is more prominent than 200 mm [2,56,57]. All the experiments are conducted with a top clearance of 50 mm and a liquid treatment capacity of 1 $m^3 \cdot h^{-1}$. The superficial gas velocities ranging from 0.038 to 0.076 $m \cdot s^{-1}$ were adopted, and the possible reverse circulation from the downcomer to the riser could be effectively prevented by using such high superficial gas velocities. Then excellent solid fluidization, liquid circulation, and solid–liquid separation performances would be achieved in the slurry reactor integrating mixing and separation.

The physical properties of the solid particles employed in this experiment are shown in Table 1.

The diameter distribution of solid particles was measured by a laser particle size analyzer BT-9300ST [58]. Each of the three-particle species was graded into two series with different median particle sizes (d_{50}), labeled as 'large-sized particle' and 'small-sized particle', respectively. The details of the particle size distribution are exhibited in Fig. 2.

The particle size distribution displays a typical Gaussian distribution as the most common style in industrialization. The contact angle, formed between the liquid–solid interface and be tangent to the liquid–gaseous interface, is an indispensable parameter to represent wettability since a better wettability of solid particles stands for a smaller contact angle. The contact angle was measured by a classic HARKE-SPCA contact angle meter. The particle sphericity was measured here by an Ergun equation [59,60] in a fluidized bed [61]:

$$\frac{\Delta P_b}{L} = 150\frac{(1-\varepsilon_b)^2}{\varepsilon_b^3(\varphi d_{50})^2}\mu_g u_g + 1.75\frac{1-\varepsilon_b}{\varepsilon_b^3 \varphi d_{50}}\rho_g u_g^2 \quad (1)$$

where φ denotes the sphericity of solid particles, dimensionless; ε_b is the porosity of solid particles in the fixed bed, dimensionless; ΔP_b represents the bed pressure drop when the air flows through the fixed bed packed with the focusing solid particles, Pa; L is defined as the height of the fixed bed, m; d_{50} signifies the mean diameter of solid particles, m; μ_g means the viscosity of the fluidizing gas, Pa·s; ρ_g refers to the density of the fluidizing gas, $kg \cdot m^{-3}$; u_g indicates the superficial gas velocity of the fluidizing gas, $m \cdot s^{-1}$.

2.2. Measuring methods

2.2.1. Overall gas holdup

The overall gas holdup in the EALR was obtained by an improved volume expansion method, measuring the difference between liquid levels with and without aeration. It is not easy to accurately record the liquid surface's height as the liquid level in the gas–liquid separator is violently fluctuated when we measure the expansion height of the fluid after aeration. An improved volume expansion method proposed by Guo *et al.* [6] was also employed here to measure the overall gas holdup [54,55]. A transparent tube with an inner diameter of 5 mm was fixed to the inner wall of the gas–liquid separator after adjusting the liquid level to a fixed height without aeration. The end of the transparent tube was wrapped with a few layers of gauze to prevent the fluctuation of the liquid expansion level, and a relatively stable hydrostatic height can be read from the transparent tube through a ruler. Consequently, the experimental error would be considerably reduced by avoiding the interferences of the bubbles and turbulence on the readings.

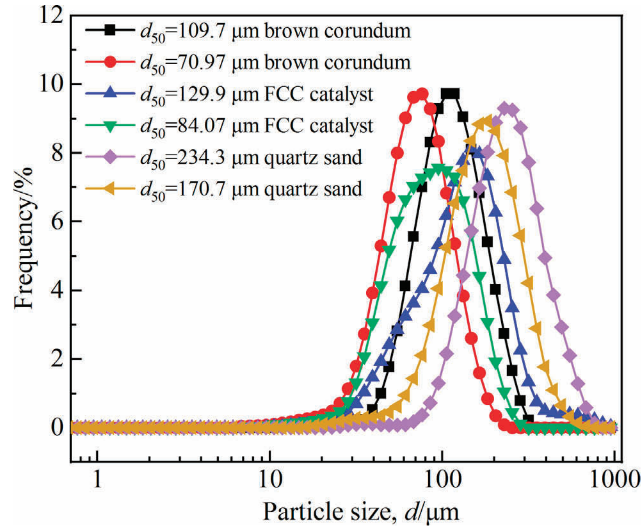

Fig. 2. The particle size distribution of experimental particles.

2.2.2. Liquid circulating velocity

A classical response technology was adopted here to measure the liquid circulating velocity in the downcomer of the slurry reactor. During the experiments, two electromagnetic flowmeters installed under the two parallel hydrocyclones individually were taken to measure the slurry circulating flow rate, with the data being tracked twice per second. 120 slurry circulating flow rate values were recorded per minute for averaging after the system ran steadily. The liquid circulating velocity was calculated by dividing the slurry flowrate, which equals the sum of the under flowrate and over flowrate in the two hydrocyclones, by the cross-sectional area of the downcomer [33,53].

2.2.3. Axial distribution of solid particles

In this experiment, the axial concentration distribution of solid particles was measured by sampling 1 L of slurry through six taps, which were installed in the riser at different axial positions, *i.e.*, 0.15, 0.65, 1.15, 1.65, 2.15, 2.65 m above the gas distributor. The taps were aligned at the position of 40 mm away from the inner wall of the riser. The mass of solid particles in the sample slurry can be acquired by filtration and drying.

To minimize the error of experimental data and further improve the reliability of the experiments, all the results were obtained by averaging at least three series of experimental data. All the experiments in this work were carried out under ambient conditions.

Table 1
Physical properties of solid particles

Solid material	d_{50}/μm	ρ/kg·m^{-3}	φ	θ/(°)	Diameter range/μm
Brown corundum	109.7 (large)	3800	0.4848	70.90	9.999–334.0
	70.97 (small)	3800	0.6402	90.23	6.449–240.4
Quartz sand	234.3 (large)	2600	0.4092	58.75	21.54–803.0
	170.7 (small)	2600	0.4591	63.16	15.50–719.4
FCC catalyst	129.9 (large)	2200	0.4460	25.57	8.961–1000
	84.07 (small)	2200	0.6209	31.41	6.449–299.3

3. Results and Discussion

3.1. Effect of solid properties on overall gas holdup

The gas holdup in the riser is the governing power source of fluid circulation between the riser and the downcomer in the EALR, determining the slurry circulating rate and mixing characteristics [62]. It is also directly related to the gas–liquid interface area and mass/heat transfer rate [63,64]. The evolutions of the overall gas holdup after adding different kinds of solid particles (*i.e.*, brown corundum, fluid catalytic cracking (FCC) catalyst, and quartz sand) at a specific solid volume loading (*i.e.*, 1.5%) with the superficial gas velocity varied from 0.038 to 0.076 $m \cdot s^{-1}$ are presented in Fig. 3.

It shows in Fig. 3 that for all the particle species, the overall gas holdup increased nearly logarithmically with the increase of the superficial gas velocity, with the slope gradually weakening. This phenomenon was due to the enhancement of bubble coalescence caused by the larger gas flux, which is analogous to the previous reports [29,33,53,55]. Compared to the three-phase systems with the small-sized solid particles, the gas holdup is more sensitive with large-sized ones when increasing the superficial gas velocity, as shown in Fig. 3. Specifically, when the superficial gas velocity increased from 0.038 to 0.076 $m \cdot s^{-1}$, the growth rates of the overall gas holdup in these three-phase systems with the small-sized particles of brown corundum, FCC catalyst, and quartz sand were 39.98%, 36.57%, and 41.01%, respectively. While adding large-sized particles into the reactor, the corresponding growth rates of the overall gas holdup increased by 48.06%, 39.85%, and 78.44%. This is due to the more substantial enhancement effect on the bubble coalescence caused by the large-sized particles, resulting in a lower initial gas holdup in the riser. Therefore, with a further increment of the superficial gas velocity, the gas holdup of the large-sized particle system will increase more dramatically than that of the small-sized particle system. This can be verified by the slope of the total gas holdup *versus* the superficial gas velocity. As pointed out by Yang and Mao [62], the slope usually shifted from a sharp linear variation with a value larger than 1.0 $s \cdot m^{-1}$ (*i.e.*, homogeneous regime) to a gradual non-linear change with a value smaller than 1.0 $s \cdot m^{-1}$ (*i.e.*, transitional or heterogeneous regime) when the bubble coalescence became evident. Therefore, more bubbles would be clustered in the system with large-sized particles at the same condition compared to the small-sized particle situation.

It is also noteworthy that the overall gas holdup in the reactor with the small-sized particles is always higher than that with the large-sized particles at the same superficial gas velocity, as presented in Fig. 3. For example, the overall gas holdup in the reactor with the small-sized particles of brown corundum, FCC catalyst, and quartz sand are individually 11.04%, 7.80%, and 29.12% higher than those with the large-sized particles at the superficial gas velocity of 0.038 $m \cdot s^{-1}$. The same phenomenon can also be found throughout the whole experiment when keeping the solid volume fraction at a constant of 1.5%. It can be concluded that the fine particles play a critical role in improving bubble breakup or reducing bubble coalescence and extending its residence time, being consistent with the previous conclusion [28,32,35].

The gas holdup difference between small-sized particle system and large-sized particle system ($\Delta\alpha_g$) under different superficial gas velocities is depicted in Fig. 4, which shows that the influence of particle size on the overall gas holdup is much smaller than that of the superficial gas velocity, especially when the large particles are added. For the same kind of particles, the gas holdup difference between the large-sized and the small-sized particles almost kept constant when the superficial gas velocity increased, especially for the solid particles of brown corundum and FCC catalyst. While for quartz sand, although the overall gas holdup is much smaller than those with the other two kinds of materials, as shown in Fig. 3, the gas holdup difference between the large-sized particles and the small-sized ones exerts a profound decline with the superficial gas velocity, mainly due to its considerable larger mean diameter

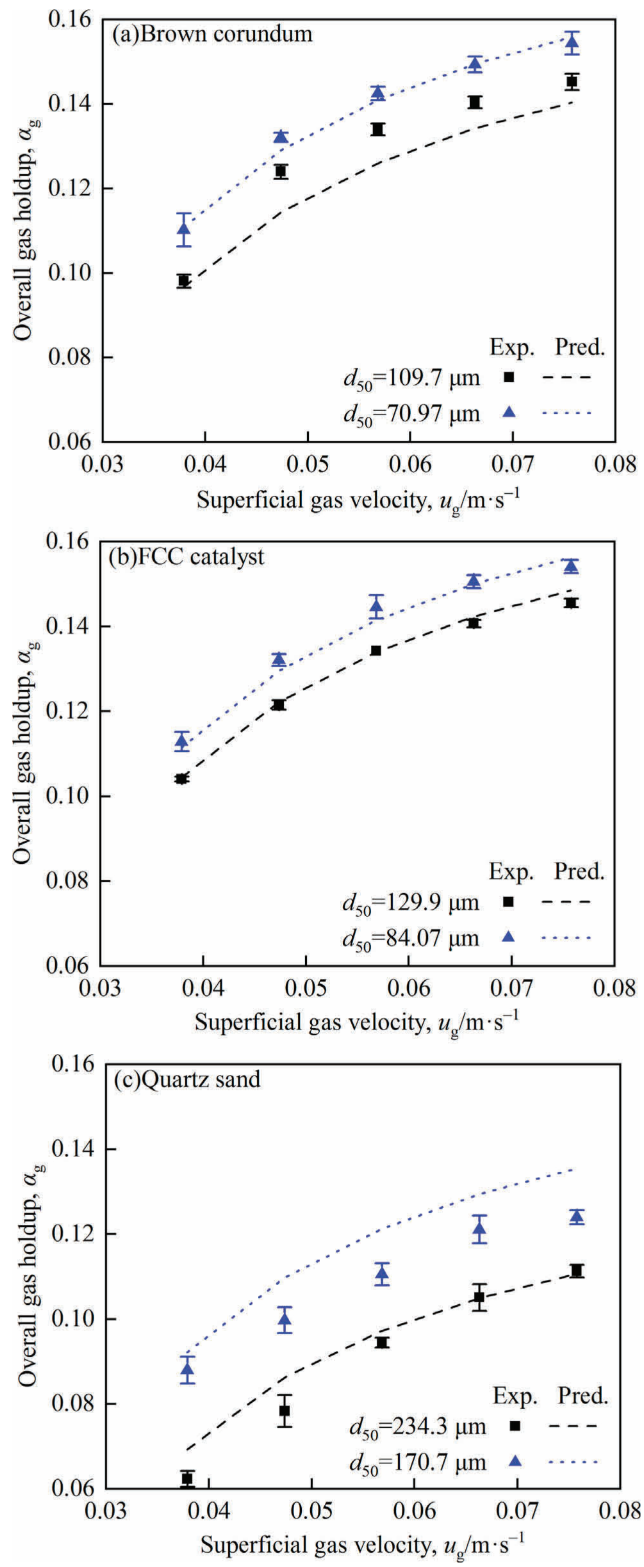

Fig. 3. Influence of the particle size on the overall gas holdup of (a) brown corundum, (b) FCC catalyst, and (c) quartz sand.

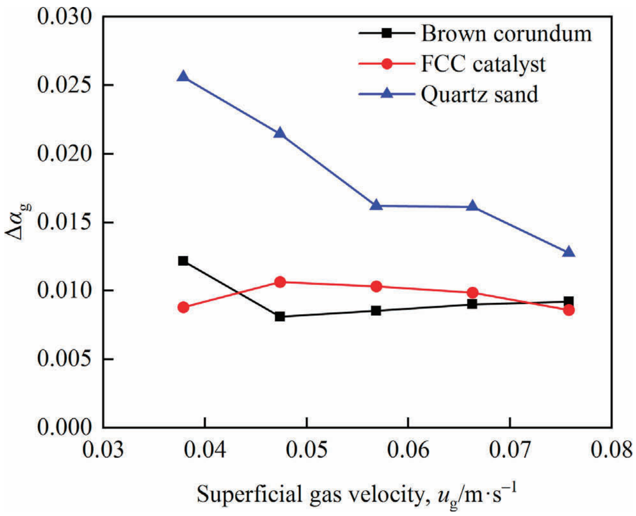

Fig. 4. Influence of particle size on the overall gas holdup difference.

than the others. It also can be seen from Fig. 4 that the gap of the overall gas holdup between large-sized and small-sized particles is reduced when the superficial gas velocity is relatively high. Taking the quartz sand as an example, the difference in total gas holdup between large-sized and small-sized particles in the slurry reactor decreases from 2.56% to 1.28% when the superficial gas velocity increases from 0.038 m·s^{-1} to 0.076 m·s^{-1}.

It can be concluded from Figs. 3 and 4 that compared to the large-sized particles, the small-sized particles can lead to a higher overall gas holdup and a more stable three-phase contacting system. Compared to the superficial gas velocity, the particle size also shows a substantial effect on the overall gas holdup, and with the further increment of superficial gas velocity, the influence of particle size on the overall gas holdup will be decayed steadily.

3.2. Effect of solid properties on liquid circulating velocity

Liquid circulating velocity (u_l) is another paramount parameter for the design, optimization, and scale-up of ALRs since it affects the reactants' mixing characteristics and residence time [65]. The liquid circulating velocity is controlled by the ratio of the driving force (*i.e.*, the height of the downcomer and the difference of gas holdup between the riser and the downcomer) to the friction resistance (*i.e.*, energy dissipation during the flow circulation) in the slurry reactor. The variation of the liquid circulating velocity against the superficial gas velocity while keeping the processing capacity of the clear liquid constant at 1 m^3·h^{-1} is shown in Fig. 5.

It shows in Fig. 5 that the liquid circulating velocity increased with the increment of the superficial gas velocity for all the particles in the experiments. For instance, when the superficial gas velocity increases from 0.038 m·s^{-1} to 0.076 m·s^{-1}, the individual liquid circulating velocity in the large-sized particle system of brown corundum, FCC catalyst, and quartz sand increases by 8.07%, 8.86%, and 15.42%, respectively. However, the corresponding values in the small-sized particle system were promoted by 10.24%, 10.42%, and 11.55%, respectively. It should be noted that the variation of the liquid circulating velocity against the superficial gas velocity is analogous to that of the overall gas holdup, which varies approximately to a logarithmical curve with a gradual diminution in slope. The reason lies in that the slurry circulation in the reactor is governed by two factors: the driven force, which is determined by the height of the downcomer and the difference of the overall gas holdup between the riser and the downcomer, and the flow resistance, which includes the resistance of gas–liquid–solid flow in the riser and that of the slurry flow in the downcomer and the two parallel hydrocyclones. It is noteworthy that this conclusion follows our previous investigation [33,53].

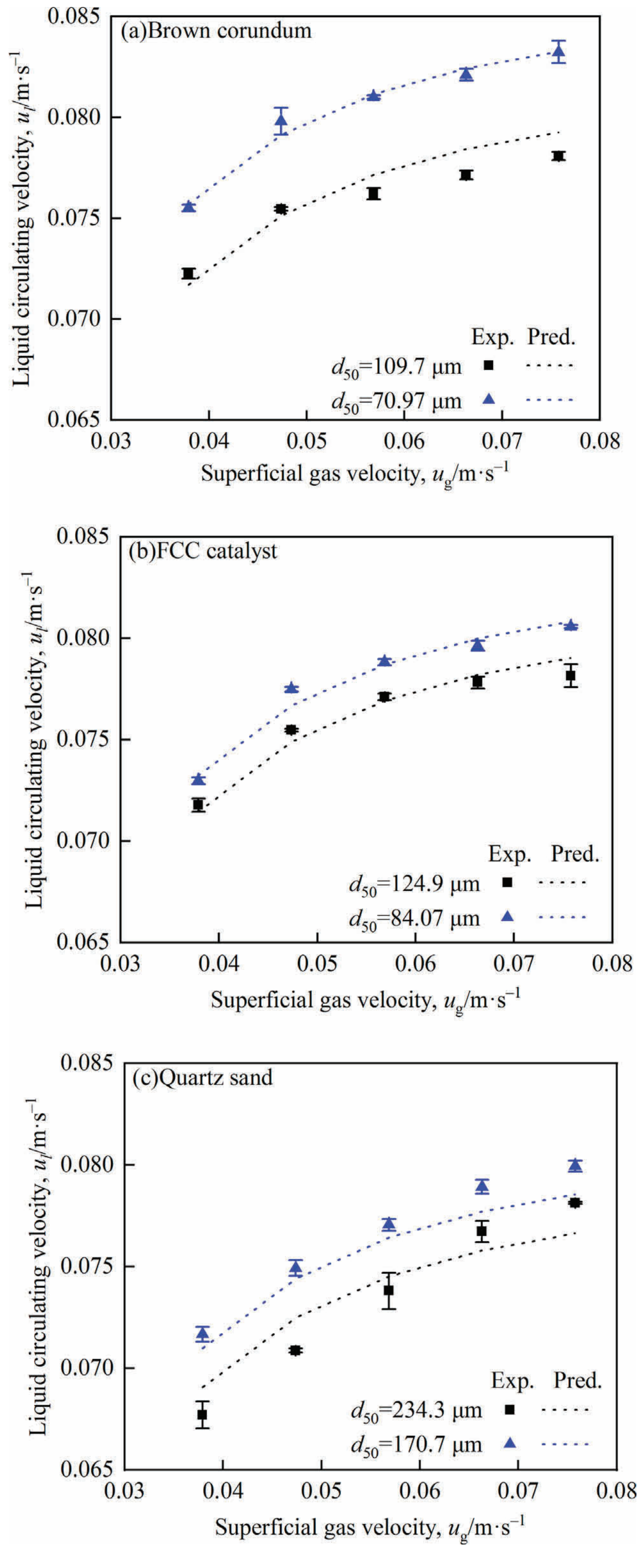

Fig. 5. Influence of particle size on the liquid circulating velocity of (a) brown corundum, (b) FCC catalyst, and (c) quartz sand.

The liquid circulating velocity varies distinctly for the same particle species when the particle size increases markedly. As illustrated in Fig. 5, the small-sized particles will give a faster slurry circulation in all the cases. For example, when the superficial gas velocity comes to 0.038 $m\cdot s^{-1}$, the liquid circulating velocities of brown corundum, FCC catalyst, and quartz sand with small median diameter are individually 4.53%, 1.66%, and 5.86% higher than those with the large-sized particle, while the corresponding values at the superficial gas velocity of 0.076 $m\cdot s^{-1}$ are 6.62%, 3.11%, and 2.32% higher, respectively. This phenomenon can also be ascribed to the enhancement of gas holdup in the riser resulting from the substantial bubble breakup with small particles [66]. In other words, the circulation driving force, *i.e.*, the gas holdup difference between the riser and the downcomer, will be strengthened by the relatively smaller bubbles in the reactor resulting from the small-sized particles.

In order to reveal the impacts of particle size on the u_l more clearly, the differences in the liquid circulation velocities between the small-sized particle system and the large-sized particle system (Δu_d) *versus* superficial gas velocity are also plotted here and displayed in Fig. 6.

For each particle species, the difference of liquid circulating velocity between small-sized and large-sized particle systems can be calculated by:

$$\Delta u_d = u_{l,sml} - u_{l,lar} = 0.296u_g + 1730.871u_g h_f^2 - 81.134h_f^2 + 2.62h_f - 58.284u_g h_f - 0.00928$$
$$R^2 = 0.96 \quad (2)$$

where $u_{l,sml}$ denotes the liquid circulation velocity of the system with the small-sized particle, while $u_{l,lar}$ stands for that with the larger one. h_f is the dimensionless particle diameter difference between the two series of particles and can be described by:

$$h_f = \frac{\sum f_{i,lar} d_{j,lar}}{d_{50,lar}} - \frac{\sum f_{i,sml} d_{j,sml}}{d_{50,sml}} \quad (3)$$

where d_j represents the mean particle diameter of each range of the testing results; f_i is the corresponding frequency proportion in each particle size tested by the laser particle size analyzer. The median particle diameters of the large and small systems here are defined as $d_{50,lar}$ and $d_{50,sml}$, respectively. It is noteworthy that the gaps of the liquid circulating velocities between the large and fine particles in the brown corundum and the FCC catalyst systems have a similar positive correlation with the superficial gas velocity, while there is an opposite effect for the quartz sand system. This phenomenon is probably due to the larger span of the mean diameter of the quartz sand (63.6 μm).

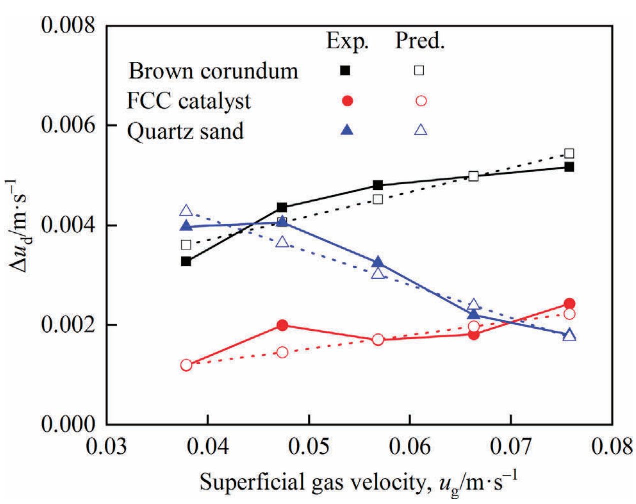

Fig. 6. Influence of particle size on the liquid circulating velocity difference.

3.3. Decoupling the impacts of solid multi-physical properties on hydrodynamics

3.3.1. Theoretical exploration foundation

The superficial gas velocity, particle density, particle size, contact angle, and sphericity are related to gas holdup and liquid circulating velocity. It has a specific guiding significance in understanding the influence of the above factors on improving the hydrodynamic properties in the EALR. However, it is unrealistic to perform univariate analysis through experiments since it is impossible to decouple one particular physical property of the solid particles from many other variations because of the inherent attribute. A regression decoupling method was proposed here to overcome the difficulties mentioned above for a profound understanding of the effects of the solid particles' physical properties on the hydrodynamic behaviors in the new EALR. The experimental data of three kinds of solid particles with different physical properties (*i.e.*, contact angle, sphericity, mean diameter, and density) under the superficial gas velocity ranging from 0.038 $m\cdot s^{-1}$ to 0.076 $m\cdot s^{-1}$ were taken to investigate the impacts of the individual property. It should be noted that an average value of the sphericity of the particles was employed here to describe the shape factor for different solid particles. From the analysis aforementioned, it can be concluded that the gas holdup and liquid circulating velocity can be expressed as a function of the following parameters:

$$\alpha_g = f(u_g, u_r, D_T, \mu, \sigma, \theta, \varphi, \rho, d_{50}) \quad (4)$$

$$u_l = g(u_g, u_r, D_T, \mu, \sigma, \theta, \varphi, \rho, d_{50}) \quad (5)$$

Since only the effects of the superficial gas velocity and the physical properties of solid particles are investigated here, Eqs. (4) and (5) can be simplified as follows:

$$\alpha_g = f(u_g, \theta, \varphi, \rho, d_{50}) \quad (6)$$

$$u_l = g(u_g, \theta, \varphi, \rho, d_{50}) \quad (7)$$

The five parameters mentioned previously are dimensionless to standardize the two semi-empirical equations. Based on the impacts of the physical properties of solid particles and superficial gas velocities on the gas holdup and liquid circulating velocity, the mathematical models are then put forward using the traditional non-linear analysis method. The evolution of the overall gas holdup and the liquid circulating velocity *versus* the solid physical properties can be well portrayed, and the semi-empirical equations are shown as follows:

$$\alpha_g = \frac{0.01428\ln(\beta/\pi)\ln Re}{\varphi^{-1.8962} Re_s^{-2.0444}} - \frac{547.6408}{Re} + 0.2206\left(\frac{\beta}{\varphi\pi Re_s}\right)^{0.01664}$$
$$R^2 = 0.94 \quad (8)$$

$$u_l = -\frac{0.004506\ln(\beta/\pi)}{\varphi^{-0.2075} Re_s^{0.02746}} + \frac{0.2008}{Re^{0.09921}} - \frac{156.3909}{Re} + \frac{0.01252\beta}{\pi\varphi Re_s}$$
$$R^2 = 0.95 \quad (9)$$

where Re ($Re = D_T u_g \rho_l/\mu$) is the Reynolds number in the riser, dimensionless; β denotes the contact angle for the solid particles ($\beta = \theta\pi/180$), dimensionless; φ represents the sphericity of the solid particles, dimensionless; Re_s means Reynolds number of particles, which is calculated by $Re_s = d_{50}u_r\rho_s/\mu$. It should be noted that the parameters in the above equations are defined as follows: D_T is the diameter of the riser, m; u_g means the operating superficial gas velocity, $m\cdot s^{-1}$; ρ_l is prescribed as the density of the fluid (*i.e.*, tap water), $kg\cdot m^{-3}$; u_r designates the liquid superficial velocity in the riser (*i.e.*, the handling capacity of the slurry reactor), $m\cdot s^{-1}$; μ is named as the liquid viscosity in the reactor, Pa·s; d_{50} is specified as the mean diameter of the solid particles, m; ρ_s is prescribed as the density of solid particles, kg·m^{-3}. The scope of these variables in the two semi-empirical equations is: 0.038 m·s^{-1} $\leq u_g \leq$ 0.076 m·s^{-1}; 25°$\leq \theta \leq$ 90°; 0.4 $\leq \varphi \leq$ 0.8; 2200 kg·m^3 $\leq \rho \leq$ 3800 kg·m^{-3}; 70 μm $\leq d_{50} \leq$ 230 μm.

The predicted overall gas holdup and liquid circulating velocities based on Eqs. (8) and (9) are compared with experimental results, and the corresponding results are illustrated in Figs. 3 and 5. It is noteworthy that the predicted values of the gas holdup and the liquid circulating velocity are all in good agreement with the experimental data, with the maximum relative errors of 11.2% and 2.3%, respectively.

3.3.2. Effect of solid properties on overall gas holdup

Based on the semi-empirical equations, a feasible and straightforward control variable method was applied to study the influence of the individual physical property of solid particles on the main hydrodynamic properties (gas holdup and liquid circulating velocity) in the new EALR. Specifically, particle physical properties such as contact angle, sphericity, mean diameter, or density are taken as variables, respectively, and 11 values are selected from the range mentioned above in the arithmetic series for calculation.

The overall gas holdup calculated *via* the proposed semi-empirical equations was adopted here to plot the tendency charts of their evolution against the physical properties of solid particles, and the corresponding results are illustrated in Fig. 7.

From Fig. 7(a), it can be seen that the overall gas holdup decreases with the increment of the solid density. This conclusion complies with that of the previous investigation [35,43], originating from the increase of the local slurry apparent viscosity and slurry density caused by solid particles, which will increase the tensile ability of bubbles and the number of big bubbles, and consequently result in a reduction in the gas holdup [2,67]. Additionally, the bubble coalescence can also be promoted by the heavy particles, which will give rise to a decrease in the overall gas holdup [40,66]. Fig. 7(a) also showed that the effect of solid density on overall gas holdup is considerable, echoing with the experimental results in Fig. 3. However, this conclusion is inconsistent with that of Freitas *et al.* [41], who supposed that the impact of solid density on the gas holdup is slight. It is mainly ascribed to the density span of the solid particles they used being too small (1023 and 1048 kg·m^{-3} for the low- and high-density particles). Though the particle density difference is also small (Lexan, 1170 kg·m^{-3}, PS, 1350 kg·m^{-3}), Guo *et al.* [42] observed an opposite phenomenon mainly because they ignored the influence of particle size (3.0–3.3 mm), which was higher by an order of magnitude than this work.

The particle size has an indispensable predominance in the gas volume fraction. As seen from Fig. 7(a), the larger the particle size, the smaller the overall gas holdup is. The negative contribution of the solid particle size on the gas holdup was also found by the majority of the scholars [31–33,54,55,66], while it is in contradiction with some others [36,37,39]. In Kelkar *et al.* [36], the researchers deemed that the particle size only affected the solid sedimentation velocity, which was an order of magnitude smaller than the liquid velocity, and the influence of particle size on the hydrodynamics was ignored. Saxena and Patel [37] employed a small reactor (ID 0.108 m) but with a much high solid holdup (10%), fine solid particles (50, 90, and 143 μm), and high superficial gas velocity (ranging from 0.02 to 0.37 m·s^{-1}), and the impacts of particle size on the gas holdup might be hidden due to the high superficial gas velocity, high solid concentration and wall effect [2]. The CFD predicted results of gas–liquid–solid-froth flow in a bubble column [39] should be verified further with the experimental data because of the well-known open question on the closure of interphase forces, turbulence, and bubble coalescence and break-up [2]. Finally, as indicated by Kelkar *et al.* [36], the impacts of solid

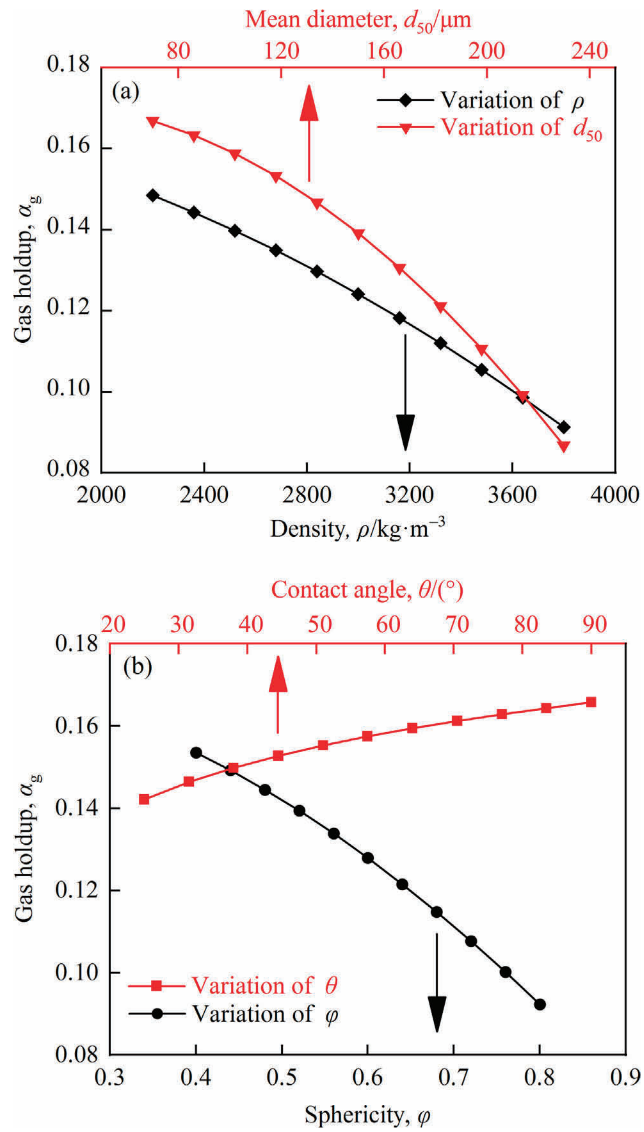

Fig. 7. Theoretical effects of the physical properties of (a) mean diameter and density and (b) sphericity and contact angle on the gas holdup.

particle size on gas holdup can also be attributed to the expansions of viscosity and density of the continuous phase with the addition of large solid particles. Additionally, as Mowla *et al.* [46] indicated, too large particles could favor the bubble break-up by cutting the big bubbles into the small ones.

When the contact angle increases, which means that the wettability of the solid particles will weaken while the hydrophobicity usually promotes, the overall gas holdup increases gradually, as indicated in Fig. 7(b). This is because the hydrophobic particles can have strong adsorption to the bubbles, which can increase the bubble mass but reduce their rising speed, leading to an increase in the overall gas holdup [48,68]. This result follows the phenomenon observed by Bhatia *et al.* [47] and conclusions obtained by Kelkar *et al.* [36].

However, this result is inconsistent with the results of other researchers [43–46]. In the work of Jamialahmadi and Mullersteinhagen [43], they found that the gas holdup with the wettable particles changed considerably when the regime turned to the slug flow regime. The bigger particle diameter (0.8–2 mm) and different flow characteristics resulting from small reactor diameter (0.152 m) and high superficial gas velocity (>0.05 m·s^{-1}) may be the main reason for the opposite conclusion. In the contribution of Kluytmans *et al.* [44], only the wettable particles of carbon were investigated, and hence it demanded more experimental data to verify that the wettable particles tended to decrease the rate of bubble coalescence. Similarly, Sarhan *et al.* [45] predicted the gas holdup in a small column (ID of 0.1 m) under lower superficial gas velocities ranging from 0.0064–0.0267 $m \cdot s^{-1}$ but at high coal solid concentrations (10%), and the solid particles may not be fully fluidized. What's more, their predicted CFD results also showed a promotion effect on the gas holdup above a certain height of the column, while a contrary trend was observed in their predicted results below that critical height. Therefore, some experimental data are highly desired. Such problems can also be found in Mowla *et al.* [46], in which a small column (ID of 15.2 cm and height of 220 cm) was used. It should be noted that the influence of the wettability of particles is much smaller than other parameters such as superficial gas velocity, particle density, *etc.*

The impacts of the solid particle shape on the hydrodynamics in the slurry reactors still lack essential investigations [66]. From Fig. 7(b), it also can be seen that the overall gas holdup decreases with the increment of sphericity, which is similar to the opinion advocated by Sastaravet *et al.* [49]. With the increment of the particle's sphericity, the particle shape becomes closer to a sphere, and consequently the fluidization quality will be promoted due to low flow resistance, while its ability to break up big bubbles will be impeded by the smooth surface [66]. As pointed out in the literature [66,69], the sharp surface of low-sphericity particles can pierce bubbles easily into more small bubbles, giving rise to a higher gas holdup. That is to say, the more the solid particle shape is close to the sphere, the lower the gas holdup will be obtained.

From the above discussion, it can be seen that the two equations can illustrate the influencing degree of each variable on the overall gas holdup and liquid circulating velocity, providing very important guidance in choosing proper catalysts for such multiphase reactors.

3.3.3. Effect of solid properties on liquid circulating velocity

The evolution of liquid circulating velocity computed by the semi-empirical equations was similarly investigated in connection with the physical properties of solid particles. As shown in Fig. 8(a), increasing particle size will reduce the liquid circulating velocity due to more energy in the system will be taken to keep the normal circulation of bigger particles, of which the terminal settling velocity increases [70]. This result is also consistent with the experimental phenomenon.

Increasing the density of solid particles also has a negative effect on the liquid circulating velocity because of the decrease of the overall gas holdup in the reactor as the density can influence the breakup and coalescence of bubbles. This phenomenon is consistent with the results of the equations proposed by Heijnen *et al.* [71] and Trilleros *et al.* [72].

According to Fig. 8(b), increasing the contact angle of particles will increase liquid circulating velocity. The reasonable explanation is that there are high polar groups inside the wettable particles that can be combined with the water, which increases the mass of the solid particles, leading to an increase in the terminal settling velocity of the solid particles and a decrease in the liquid circulating velocity. Increasing the sphericity of particles will decrease the driving force because of uniform fluidization, resulting in a diminution of the liquid circulating velocity [73]. Furthermore, the increment of sphericity of solid particles is favorable to bubble coalescence and generates many large bubbles that escape quickly from the system. In addition, the effect of solid particle properties on the liquid circulating velocity is almost following that on the overall gas holdup, which acts as the significant power source for the slurry circulation in the ALRs.

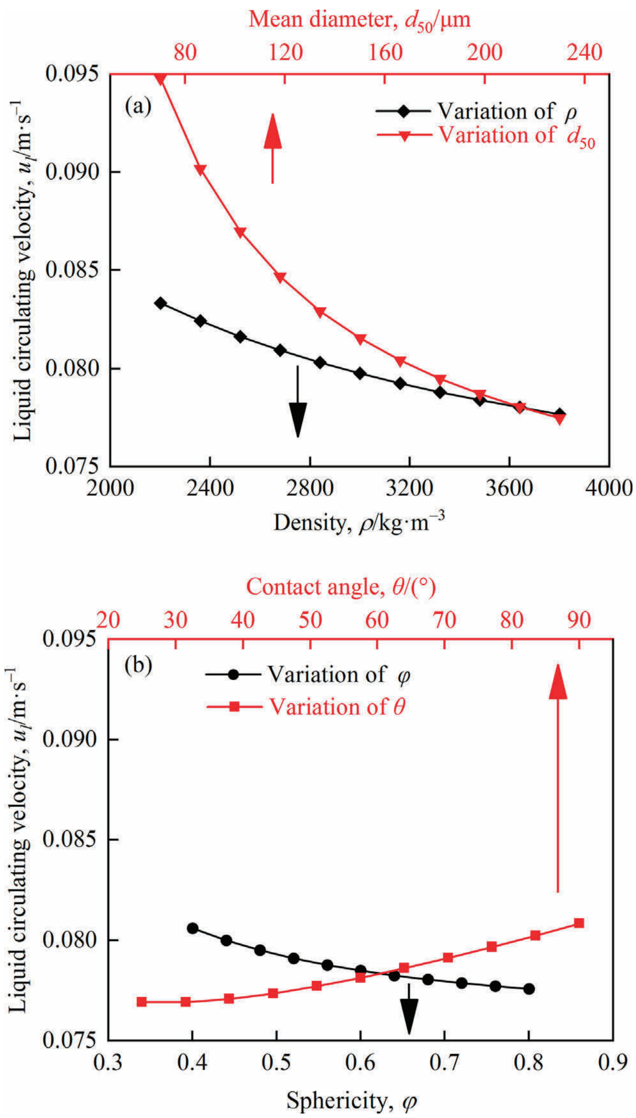

Fig. 8. Theoretical effects of the particle physical properties of (a) mean diameter and density, (b) sphericity and contact angle on the liquid circulating velocity.

3.4. Axial solid concentration distribution

The axial concentration distribution of the solid particles is an indispensable parameter to index the mixing extent of multiphase flow in the ALRs. The non-uniformities of the solid particles are usually caused by solid sedimentation or the formation of large bubbles [74], which is critical to the mass/heat transfer in the slurry reactors. The axial concentration distribution of solid particles in the riser was investigated with the solid volume fraction of 1.5% at the superficial gas velocity of 0.038, 0.057, and 0.076 $m \cdot s^{-1}$, respectively. The experimental values were attained by averaging at least three measurements, whose error of experimental data for different batches was within 11%, and the corresponding results are depicted in Fig. 9.

It can be seen from Fig. 9 that for all the solid particles investigated in this work, the uniformity of the axial solid concentration along the riser increased with the increase of superficial gas velocity, which was similar to the previous conclusion [53]. This can be ascribed to the decrease of solid deposition in the inclined tube, hidden dead zone, and corner areas of the connection between the hydrocyclones and the riser. However, the solid concentration increment becomes less when the superficial gas velocity increases

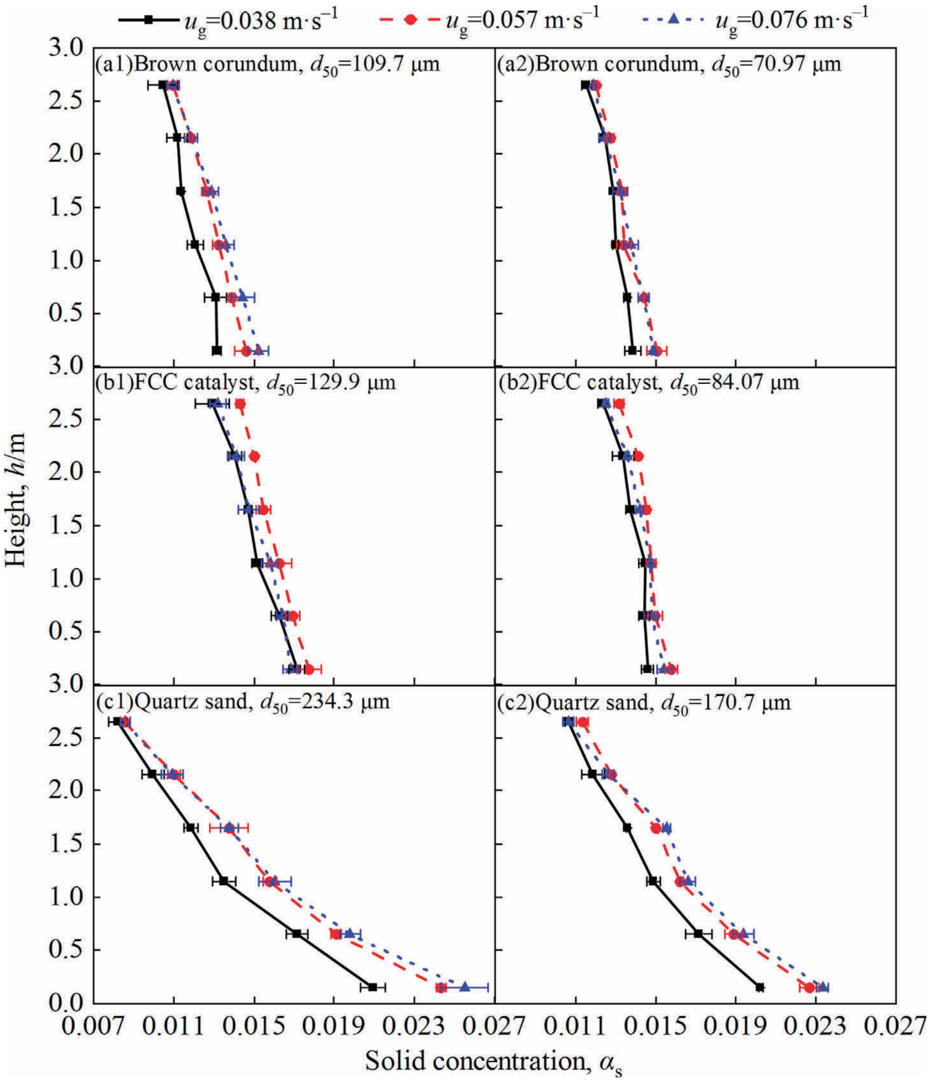

Fig. 9. Axial solid concentration distribution of different solid particles: brown corundum (a1, a2); FCC catalyst (b1, b2); quartz sand (c1, c2).

from 0.057 to 0.076 m·s^{-1} than that from 0.038 to 0.057 m·s^{-1}. That is to say, the solid concentration curves under the u_g of 0.057 m·s^{-1} and 0.076 m·s^{-1} were very close, which is mainly due to the effect of superficial gas velocity reaching its limits to play the leading role, indicating that there is an optimal superficial gas velocity for the mixing of the slurry reactors.

Interestingly, when the particle size increases, the variation of the solid concentration was more prominent with the small-sized particle system than that with the large-sized ones, as seen in Fig. 9. It can be inferred that the fluidization quality of the small-sized particle system is much better, which could benefit the uniform distribution of the solid catalysts. Quartz sand showed a remarkably higher solid concentration at the bottom of the riser than that of the top, which is quite different from FCC catalyst and brown corundum. This phenomenon is due to the increase in particle settling velocity with the bigger particles, being consistent with the results of Zhang [51].

It should be noted that for different particle species, as seen in Fig. 9, the solid concentration spans are quite different, expressing a significant variation of the local solid concentration distribution. Therefore, the mixing index of solid particles in the riser in such a three-phase system can be quantitatively defined as D_α, which can be depicted as:

$$D_\alpha = \frac{\alpha_{s,max} - \alpha_{s,min}}{\alpha_{s,max}} = 1 - \frac{\alpha_{s,min}}{\alpha_{s,max}} \tag{10}$$

where $\alpha_{s,max}$ and $\alpha_{s,min}$ are the maximum and the minimum solid concentration in the riser, respectively. Correspondingly, the value of D_α at each superficial gas velocity was calculated and illustrated in Fig. 10.

Obviously, D_α increased with the superficial gas velocity according to Fig. 10, resulting from the increasingly violent mixing caused by the big bubbles. So D_α can reflect the turbulent flow in the riser since the bigger the D_α is, the fiercer mixing appears. It should be noted that for the brown corundum and the FCC catalyst, the D_α is much smaller than that of quartz sand (shown in Fig. 10), but the solid concentration distribution along the riser exhibited more uniform as Fig. 9 expressed. It is due to the decrease of the solid concentration differential (*i.e.*, the term of $\alpha_{s,min}/\alpha_{s,max}$ approaching 1), originating from the strong disturbance when gas flux increases. Hence, the D_α can also reflect the uniformity of the slurry in the riser. Though it has been verified that the dispersion coefficient of the solid particles would be promoted by increasing superficial gas velocity [51], it can be deduced from the above discussion that the violent mixing does not guarantee good dispersity, which

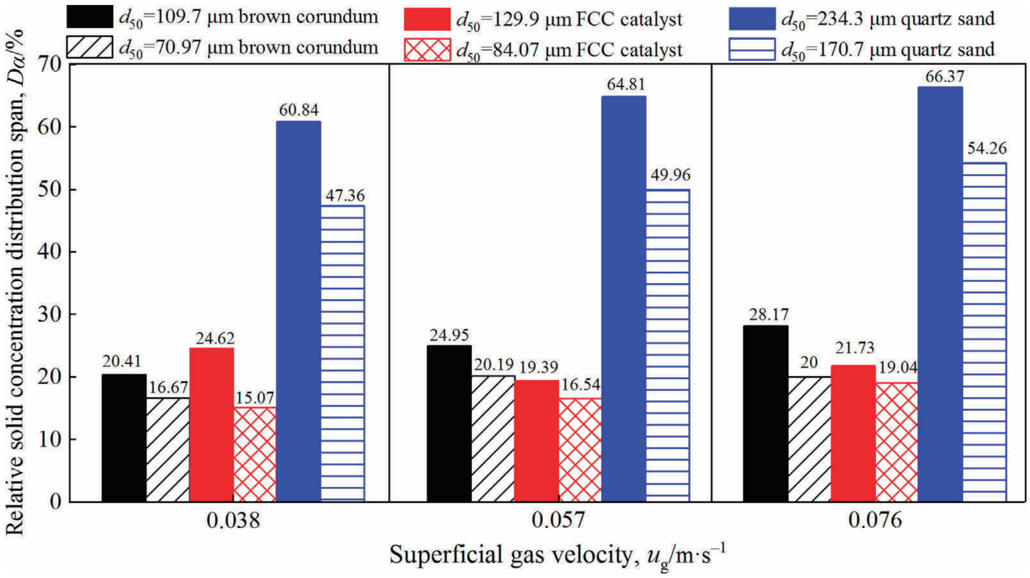

Fig. 10. The effect of solid particle size and density on mixing index (D_α) at different superficial gas velocities.

is very important for the optimal design and efficient operation of such slurry reactors.

As for the same particle species, D_α decreases with reducing particles size, as shown in Fig. 10, which is due to the diminution of solid settling velocity [50] and reduction of bubble coalescence [35]. Furthermore, by comparing the axial concentration distribution of FCC catalyst and brown corundum, whose mean diameters (*i.e.*, 129.9 and 109.7 μm) are close but particle densities (*i.e.*, 2200 and 3800 kg·m^{-3}) are remarkably different, it can be deemed that decreasing the density of the solid particles resulted in an increment of the uniformity in the axial concentration distribution.

4. Conclusions

The complex influences of particle physical properties, including particle size, density, wettability, and sphericity, on the hydrodynamic performances and axial solids concentration distribution in the new EALR integrated mixing and separation had been thoroughly investigated. Experimental results demonstrated that the solid physical properties had a substantial impact on the hydrodynamics behaviors, and two semi-empirical equations were proposed and validated to be in good agreement with the experimental data. Further investigation was theoretically conducted, and the individual influence of such particle properties was decoupled in macro- and micro-scale.

The overall gas holdup decreased with the increase of particle size, density, and sphericity due to a more significant bubble breakup, but increased with contact angle due to the promoting absorption of particles onto the bubble surface. The liquid circulating velocity was influenced similarly to the overall gas holdup, which acted as its fundamental driving force.

The influence of particle size distribution on the liquid circulating velocity was investigated for the first time, and a correlation is proposed by defining the dimensionless particle diameter difference (h_f). The axial solid concentration distribution along the riser was promoted by increasing the superficial gas velocity, resulting in a strengthened mixing degree of the slurry. The mixing index showed that the dispersion of solids could be intensified when smaller or less dense particles were added into such systems, and more uniform mixtures could be obtained. This work provides essential guidance for the design, optimization, and scale-up of the new EALR.

Declaration of Competing Interest

The authors declare that they have no known competing financial interests or personal relationships that could have appeared to influence the work reported in this paper.

Acknowledgements

This work was supported by the National Natural Science Foundation of China (21878318, 22108285), the DNL Cooperation Fund, CAS (DNL201902), "Transformational Technologies for Clean Energy and Demonstration", Strategic Priority Research Program of the Chinese Academy of Sciences (CAS) (XDA21060400), Shandong Energy Institute, Single-Cell Center Project (SCZ-16, SCZ-17), and Director Innovation Fund of Synthetic Biology Technology Innovation Center of Shandong Province (sdsynbio-2020-ZH-02).

References

[1] Q.S. Huang, C. Yang, G.Z. Yu, Z.S. Mao, 3-D simulations of an internal airlift loop reactor using a steady two-fluid model, *Chem. Eng. Technol.* 30 (7) (2007) 870–879.
[2] S.J. Geng, Z.S. Mao, Q.S. Huang, C. Yang, Process intensification in pneumatically agitated slurry reactors, *Engineering* 7 (3) (2021) 304–325.
[3] C.Q. Cao, S.Q. Dong, Q.J. Guo, Experimental and numerical simulation for gas–liquid phases flow structure in an external-loop airlift reactor, *Ind. Eng. Chem. Res.* 46 (22) (2007) 7317–7327.
[4] Q.S. Huang, C. Yang, G.Z. Yu, Z.S. Mao, Sensitivity study on modeling an internal airlift loop reactor using a steady 2D two-fluid model, *Chem. Eng. Technol.* 31 (12) (2008) 1790–1798.
[5] Q.S. Huang, W.P. Zhang, C. Yang, Modeling transport phenomena and reactions in a pilot slurry airlift loop reactor for direct coal liquefaction, *Chem. Eng. Sci.* 135 (2015) 441–451.
[6] X. Guo, L.S. Yao, Q.S. Huang, Aeration and mass transfer optimization in a rectangular airlift loop photobioreactor for the production of microalgae, *Bioresour. Technol.* 190 (2015) 189–195.
[7] Q.S. Huang, F.H. Jiang, L.Z. Wang, C. Yang, Design of photobioreactors for mass cultivation of photosynthetic organisms, *Engineering* 3 (3) (2017) 318–329.
[8] T.F. Wang, J.F. Wang, Y. Jin, Slurry reactors for gas-to-liquid processes: A review, *Ind. Eng. Chem. Res.* 46 (18) (2007) 5824–5847.
[9] R. Guettel, U. Kunz, T. Turek, Reactors for Fischer-Tropsch synthesis, *Chem. Eng. Technol.* 31 (5) (2008) 746–754.

[10] R. Krishna, S.T. Sie, Design and scale-up of the Fischer-Tropsch bubble column slurry reactor, *Fuel Process. Technol.* 64 (1–3) (2000) 73–105.
[11] M.V. Kulikova, O.S. Dement'eva, S.O. Ilyin, S.N. Khadzhiev, Formation and catalytic behavior of fine iron-containing composite Fischer–Tropsch catalysts in a slurry reactor, *Pet. Chem.* 57 (14) (2017) 1318–1325.
[12] Z.B. Chen, H.C. Min, D.X. Hu, H.C. Wang, Y.Y. Zhao, Y.B. Cui, X.J. Zou, P. Wu, H. Ge, K.Y. Luo, L.F. Zhang, W.Y. Liu, Performance of a novel multiple draft tubes airlift loop membrane bioreactor to treat ampicillin pharmaceutical wastewater under different temperatures, *Chem. Eng. J.* 380 (2020) 122521.
[13] A.H. Essadki, M. Bennajah, B. Gourich, C. Vial, M. Azzi, H. Delmas, Electrocoagulation/electroflotation in an external-loop airlift reactor—Application to the decolorization of textile dye wastewater: A case study, *Chem. Eng. Process. Process. Intensif.* 47 (8) (2008) 1211–1223.
[14] S.H. Ammar, A.S. Akbar, Oilfield produced water treatment in internal-loop airlift reactor using electrocoagulation/flotation technique, *Chin. J. Chem. Eng.* 26 (4) (2018) 879–885.
[15] Z.H. Deng, T.F. Wang, Z.W. Wang, Hydrodesulfurization of diesel in a slurry reactor, *Chem. Eng. Sci.* 65 (1) (2010) 480–486.
[16] H.L. Tung, S.Y. Chiou, C.C. Tu, W.T. Wu, An airlift reactor with double net draft tubes and its application in fermentation, *Bioprocess Eng.* 17 (1) (1997) 1–5.
[17] Q.S. Huang, L.S. Yao, T.Z. Liu, J. Yang, Simulation of the light evolution in an annular photobioreactor for the cultivation of Porphyridium cruentum, *Chem. Eng. Sci.* 84 (2012) 718–726.
[18] Q.S. Huang, T.Z. Liu, J. Yang, L.S. Yao, L.L. Gao, Evaluation of radiative transfer using the finite volume method in cylindrical photoreactors, *Chem. Eng. Sci.* 66 (17) (2011) 3930–3940.
[19] C. Junghanns, J.F. Neumann, D. Schlosser, Application of the aquatic fungus *Phoma* sp. (DSM22425) in bioreactors for the treatment of textile dye model effluents, *J. Chem. Technol. Biotechnol.* 87 (9) (2012) 1276–1283.
[20] M.H. Siegel, C.W. Robinson, Application of airlift gas–liquid–solid reactors in biotechnology, *Chem. Eng. Sci.* 47 (13–14) (1992) 3215–3229.
[21] A. Gaikwad, Direct oxidation of hydrogen to hydrogen peroxide over Pd-containing fluorinated or sulfated Al_2O_3, ZrO_2, CeO_2, ThO_2, Y_2O_3 and Ga_2O_3 catalysts in stirred slurry reactor at ambient conditions, *J. Mol. Catal. A Chem.* 181 (1–2) (2002) 143–149.
[22] E.H. Stitt, Alternative multiphase reactors for fine chemicals, *Chem. Eng. J.* 90 (1–2) (2002) 47–60.
[23] W. Strasser, A. Wonders, Hydrokinetic optimization of commercial scale slurry bubble column reactor, *AIChE J.* 58 (3) (2012) 946–956.
[24] R. Roscoe, The viscosity of suspensions of rigid spheres, *Br. J. Appl. Phys.* 3 (8) (1952) 267–269.
[25] A.S. Khare, J.B. Joshi, Effect of fine particles on gas hold-up in three-phase sparged reactors, *Chem. Eng. J.* 44 (1) (1990) 11–25.
[26] H. Li, A. Prakash, A. Margaritis, M.A. Bergougnou, Effects of micron-sized particles on hydrodynamics and local heat transfer in a slurry bubble column, *Powder Technol.* 133 (1–3) (2003) 171–184.
[27] M. Milivojevic, S. Pavlou, B. Bugarski, Liquid velocity in a high-solids-loading three-phase external-loop airlift reactor, *J. Chem. Technol. Biotechnol.* 87 (11) (2012) 1529–1540.
[28] S. Rabha, M. Schubert, M. Wagner, D. Lucas, U. Hampel, Bubble size and radial gas hold-up distributions in a slurry bubble column using ultrafast electron beam X-ray tomography, *AIChE J.* 59 (5) (2013) 1709–1722.
[29] M.L. Liu, T.W. Zhang, T.F. Wang, W. Yu, J.F. Wang, Experimental study and modeling on liquid dispersion in external-loop airlift slurry reactors, *Chem. Eng. J.* 139 (3) (2008) 523–531.
[30] E.M. Lakhdissi, A. Fallahi, C. Guy, J. Chaouki, Effect of solid particles on the volumetric gas liquid mass transfer coefficient in slurry bubble column reactors, *Chem. Eng. Sci.* 227 (2020) 115912.
[31] E.M. Lakhdissi, I. Soleimani, C. Guy, J. Chaouki, Simultaneous effect of particle size and solid concentration on the hydrodynamics of slurry bubble column reactors, *AIChE J.* 66 (2) (2020) e16813.
[32] S. Kara, B.G. Kelkar, Y.T. Shah, N.L. Carr, Hydrodynamics and axial mixing in a three-phase bubble column, *Ind. Eng. Chem. Process. Des. Dev.* 21 (4) (1982) 584–594.
[33] T. Yang, S.J. Geng, F. Gao, T.B. He, J.C. Cheng, Q.S. Huang, C. Yang, Investigation of hydrodynamics and mass transfer in an internal loop airlift slurry reactor integrating mixing and separation, *Sep. Purif. Technol.* 259 (2021) 118209.
[34] E. Sada, H. Kumazawa, C.H. Lee, Influences of suspended fine particles on gas holdup and mass transfer characteristics in a slurry bubble column, *AIChE J.* 32 (5) (1986) 853–856.
[35] M. Götz, J. Lefebvre, F. Mörs, R. Reimert, F. Graf, T. Kolb, Hydrodynamics of organic and ionic liquids in a slurry bubble column reactor operated at elevated temperatures, *Chem. Eng. J.* 286 (2016) 348–360.
[36] B.G. Kelkar, Y.T. Shah, N.L. Carr, Hydrodynamics and axial mixing in a three-phase bubble column. Effects of slurry properties, *Ind. Eng. Chem. Process. Des. Dev.* 23 (2) (1984) 308–313.
[37] S.C. Saxena, B.B. Patel, Heat transfer and hydrodynamic investigations in a baffled bubble column: Air–water–glass bead system, *Chem. Eng. Commun.* 98 (1) (1990) 65–88.
[38] W.L. Li, W.Q. Zhong, B.S. Jin, Y. Lu, T.T. He, Flow patterns and transitions in a rectangular three-phase bubble column, *Powder Technol.* 260 (2014) 27–35.
[39] A.R. Sarhan, J. Naser, G. Brooks, Effects of particle size and concentration on bubble coalescence and froth formation in a slurry bubble column, *Particuology* 36 (2018) 82–95.
[40] M.J. Bly, R.M. Worden, Gas holdup in a three-phase fluidized-bed bioreactor, *Appl. Biochem. Biotechnol.* 24–25 (1) (1990) 553–564.
[41] C. Freitas, M. Fialová, J. Zahradnik, J.A. Teixeira, Hydrodynamics of a three-phase external-loop airlift bioreactor, *Chem. Eng. Sci.* 55 (21) (2000) 4961–4972.
[42] Y.X. Guo, M.N. Rathor, H.C. Ti, Hydrodynamics and mass transfer studies in a novel external-loop airlift reactor, *Chem. Eng. J.* 67 (3) (1997) 205–214.
[43] M. Jamialahmadi, H. Müller-Steinhagen, Effect of solid particles on gas hold-up in bubble columns, *Can. J. Chem. Eng.* 69 (1) (1991) 390–393.
[44] J.H.J. Kluytmans, B.F.M. Kuster, J.C. Schouten, Gas holdup in a slurry bubble column: Influence of electrolyte and carbon particles, *Ind. Eng. Chem. Res.* 40 (23) (2001) 5326–5333.
[45] A.R. Sarhan, J. Naser, G. Brooks, CFD analysis of solid particles properties effect in three-phase flotation column, *Sep. Purif. Technol.* 185 (2017) 1–9.
[46] A. Mowla, M.A. Ioannidis, Effect of particle wettability on the hydrodynamics of three-phase fluidized beds subject to foaming, *Powder Technol.* 374 (2020) 58–69.
[47] V.K. Bhatia, K.A. Evans, N. Epstein, P. Dakshinamurty, Effect of solids wettability on expansion of gas–liquid fluidized beds, *Ind. Eng. Chem. Process. Des. Dev.* 11 (1) (1972) 151–152.
[48] A. Vazirizadeh, J. Bouchard, Y. Chen, Effect of particles on bubble size distribution and gas hold-up in column flotation, *Int. J. Miner. Process.* 157 (2016) 163–173.
[49] P. Sastaravet, S. Bun, K. Wongwailikhit, N. Chawaloesphonsiya, M. Fujii, P. Painmanakul, Relative effect of additional solid media on bubble hydrodynamics in bubble column and airlift reactors towards mass transfer enhancement, *Processes* 8 (6) (2020) 713.
[50] P. Mena, A. Ferreira, J.A. Teixeira, F. Rocha, Effect of some solid properties on gas–liquid mass transfer in a bubble column, *Chem. Eng. Process. Process. Intensif.* 50 (2) (2011) 181–188.
[51] K. Zhang, Axial solid concentration distribution in tapered and cylindrical bubble columns, *Chem. Eng. J.* 86 (3) (2002) 299–307.
[52] H.M. Abdullah, Study of axial solid concentration distribution in slurry bubble columns, *Energy Procedia* 157 (2019) 1537–1545.
[53] S.J. Geng, Z. Li, H.Y. Liu, C. Yang, F. Gao, T.B. He, Q.S. Huang, Hydrodynamics and mass transfer in a slurry external airlift loop reactor integrating mixing and separation, *Chem. Eng. Sci.* 211 (2020) 115294.
[54] T. Yang, S.J. Geng, C. Yang, Q.S. Huang, Hydrodynamics and mass transfer in an internal airlift slurry reactor for process intensification, *Chem. Eng. Sci.* 184 (2018) 126–133.
[55] H.Y. Liu, Z. Li, S.J. Geng, F. Gao, T.B. He, Q.S. Huang, Influences of top clearance and liquid throughput on the performances of an external loop airlift slurry reactor integrated mixing and separation, *Chin. J. Chem. Eng.* 28 (6) (2020) 1514–1521.
[56] S. Sasaki, K. Uchida, K. Hayashi, A. Tomiyama, Effects of column diameter and liquid height on gas holdup in air–water bubble columns, *Exp. Therm. Fluid Sci.* 82 (2017) 359–366.
[57] P.M. Wilkinson, A.P. Spek, L.L. van Dierendonck, Design parameters estimation for scale-up of high-pressure bubble columns, *AIChE J.* 38 (4) (1992) 544–554.
[58] H.Y. Liu, Q. Yin, Q.S. Huang, S.J. Geng, T.B. He, A.Q. Chen, Experimental investigation on interaction of vortex finder diameter and length in a small hydrocyclone for solid–liquid separation, *Sep. Sci. Technol.* 57 (5) (2022) 733–748.
[59] S. Ergun, Fluid flow through packed columns, *Chem. Eng. Prog.* 48 (2) (1952) 89–94.
[60] N. Dukhan, P. Patel, Equivalent particle diameter and length scale for pressure drop in porous metals, *Exp. Therm. Fluid Sci.* 32 (5) (2008) 1059–1067.
[61] Q.H. Zhu, W.K. Hao, J.L. Tao, Q.S. Huang, C. Yang, State dependence of magnetized fluidized bed reactor on operation mode, *Chem. Eng. J.* 407 (2021) 127211.
[62] C. Yang, Z.S. Mao, Numerical Simulation of Multiphase Reactors with Continuous Liquid Phase, Elsevier, Oxford (2014).
[63] C.Q. Cao, Y.N. Zhao, S.Q. Dong, Q.J. Guo, Dimensional similitude for scale-up of hydrodynamics in a gas–liquid–(solid) EL-ALR, *Chem. Eng. Sci.* 64 (23) (2009) 4992–5001.
[64] J.L. Tao, J.G. Huang, S.J. Geng, F. Gao, T.B. He, Q.S. Huang, Experimental investigation of hydrodynamics and mass transfer in a slurry multistage internal airlift loop reactor, *Chem. Eng. J.* 386 (2020) 122769.
[65] K.H. Choi, W.K. Lee, Circulation liquid velocity, gas holdup and volumetric oxygen transfer coefficient in external-loop airlift reactors, *J. Chem. Technol. Biotechnol.* 56 (1) (1993) 51–58.
[66] H. Yang, A.Q. Chen, S.J. Geng, J.C. Cheng, F. Gao, Q.S. Huang, C. Yang, Influences of fluid physical properties, solid particles, and operating conditions on the hydrodynamics in slurry reactors, *Chin. J. Chem. Eng.* 44 (2022) 51–71.
[67] H. Xiao, S.J. Geng, A.Q. Chen, C. Yang, F. Gao, T.B. He, Q.S. Huang, Bubble formation in continuous liquid phase under industrial jetting conditions, *Chem. Eng. Sci.* 200 (2019) 214–224.
[68] A. Uribe-Salas, P. de Lira-Gómez, R. Pérez-Garibay, F. Nava-Alonso, L. Magallanes-Hernández, C. Lara-Valenzuela, Overloading of gas bubbles in column flotation of coarse particles and effect upon recovery, *Int. J. Miner. Process.* 71 (1–4) (2003) 167–178.
[69] K. Wongwailikhit, P. Warunyuwong, N. Chawaloesphonsiya, N. Dietrich, G. Hébrard, P. Painmanakul, Gas sparger orifice sizes and solid particle characteristics in a bubble column—Relative effect on hydrodynamics and mass transfer, *Chem. Eng. Technol.* 41 (3) (2018) 461–468.
[70] W.J. Lu, S.J. Hwang, C.M. Chang, Liquid velocity and gas holdup in three-phase internal loop airlift reactors with low-density particles, *Chem. Eng. Sci.* 50 (8) (1995) 1301–1310.

[71] J.J. Heijnen, J. Hols, R.G.J.M. van der Lans, H.L.J.M. van Leeuwen, A. Mulder, R. Weltevrede, A simple hydrodynamic model for the liquid circulation velocity in a full-scale two- and three-phase internal airlift reactor operating in the gas recirculation regime, *Chem. Eng. Sci.* 52 (15) (1997) 2527–2540.
[72] J. Trilleros, R. Díaz, P. Redondo, Three-phase airlift internal loop reactor: Correlations for predicting the main fluid dynamic parameters, *J. Chem. Technol. Biotechnol.* 80 (5) (2005) 515–522.
[73] A. Riazi, U. Türker, The drag coefficient and settling velocity of natural sediment particles, *Comput. Part. Mech.* 6 (3) (2019) 427–437.
[74] P.C. Mena, M.C. Ruzicka, F.A. Rocha, J.A. Teixeira, J. Drahoš, Effect of solids on homogeneous–heterogeneous flow regime transition in bubble columns, *Chem. Eng. Sci.* 60 (22) (2005) 6013–6026.